Stabilization of an Inverted Pendulum with Base Arcing about a Horizontal Axis

by

Ziaieh C Sobhani

Submitted to the Department of Mechanical Engineering
in partial fulfillment of the requirements for the degree of

Bachelor of Science in Mechanical Engineering

at the

MASSACHUSETTS INSTITUTE OF TECHNOLOGY

February 2003

Author .....
Department of Mechanical Engineering
August 11, 2003

Certified by .....
Derek Rowell
Professor
Thesis Supervisor

Accepted by .....
Ernest Cravalho
Chairman, Department Undergraduate Thesis Committee

Stabilization of an Inverted Pendulum with Base Arcing about a Horizontal Axis

by

Ziaieh C Sobhani

Submitted to the Department of Mechanical Engineering
on August 11, 2003, in partial fulfillment of the
requirements for the degree of
Bachelor of Science in Mechanical Engineering

Abstract

This study sought to create an inverted pendulum control system using simple analog components for demonstration in an undergraduate controls lab. Integration with MIT's 2.010 motor control lab necessitated the stabilization of an inverted pendulum with its base travelling in an arc about a horizontal axis.

A detailed dynamic model of this system was derived. A full state feedback approach was modelled and analyzed using MATLAB's Simulink. A small pendulum was constructed and mounted to a motor in the 2.010 lab. An analog control circuit was designed and tested.

Stabilization was unsuccessful primarily due to nonlinear friction effects in the motor. The effects of the motor dead zone were examined in the Simulink model and future improvements are discussed.

Thesis Supervisor: Derek Rowell
Title: Professor

Acknowledgments

I would like to thank Prof. Rowell for his generous time discussing control theory, circuits, and Simulink. He also deserves credit for suggesting the 2.010 lab platform as a basis for the inverted pendulum. This system was considerably more interesting and simpler to construct as a result.

I would like to thank Mariano Alvira for the generous use of his oscilliscope, resistor bank, and time discussing circuits with me; Dave Mellis and Sedina Tsikata for lots of food and distractions; Katie Lilienkamp for her awesome example and willingness to discuss the inverted pendulum in any isle of Star; Andrei Maces for the crash course in LaTeX; and Josh Pieper for listening and reassuring me about my circuits.

I especially want to thank Michelle Nadermann for typing for me (when I developed RSI) and generally being one of the greatest friends ever.

Unicycle Forever!

—Zia

Contents

List of Figures

List of Tables

Chapter 1

Introduction

The inverted pendulum is a classic controls problem commonly covered in introductory controls and dynamics classes. Many people have solved the inverted pendulum problem, the most notable recent example being Dean Kamen's Segway. Many modern inverted pendulums use gyroscopic sensors, expensive optical encoders and accelerometers in tandem with microprocessors or full-blown computers to implement their control algorithms. While the sophistication of these sensors and computing power have their advantages, they make the control problem intangible to students with only a rudimentary knowledge of these sensors and advanced controls techniques.

Thus, while the problem of stabilizing the inverted pendulum on a cart is not a new one, the challenge undertaken here was to control an inverted pendulum using simple analog components such as potentiometers and operational amplifiers, thus demonstrating the solution in a manner more accessible to introductory controls students. To further this goal, the inverted pendulum designed here used a motor currently in the MIT Mechanical Engineering undergraduate motor control lab. Using this motor to control the base of the inverted pendulum increases the potential for integrating this project into the controls lab and making this solution accessible to students.

Integrating the pendulum with the 2.010 controls lab meant moving beyond the classic linear inverted pendulum problem to stabilize a pendulum with its base travelling in an arc about a horizontal axis.

Chapter 2 briefly presents the classic inverted pendulum and derives the dynamic

model of the inverted pendulum with an arcing base. Chapter 3 discusses the full state feedback approach and the MATLAB simulations of the pendulum. Chapter 4 details the mechanical system, including the 2.010 lab platform, the pendulum designed, and circuitry added to obtain additional feedback signals necessary for full state feedback. Chapter 5 describes the setup required and the procedure for testing and debugging and the attempt to compensate for friction. Chapter 6 discusses why this stabilization attempt was unsuccessful and recommendations to overcome damping effects in the future.

Chapter 2

Dynamics

2.1 Overview of the Classic Inverted Pendulum

The inverted pendulum on a cart is a classic problem in dynamics and controls. The basic system is represented here in Figure 2-1. The pendulum mass, m, is supported by a rigid rod of length L. The rod rotates in the xy plane about the pivot P on the cart. The cart is of mass M and moves along the x-axis. The challenge is to prevent the pendulum from falling by controlling the input force, F, on the base of the pendulum. The system can be fully described by the coordinates θ for the pendulum angle and x_P to measure the horizontal position of the cart.

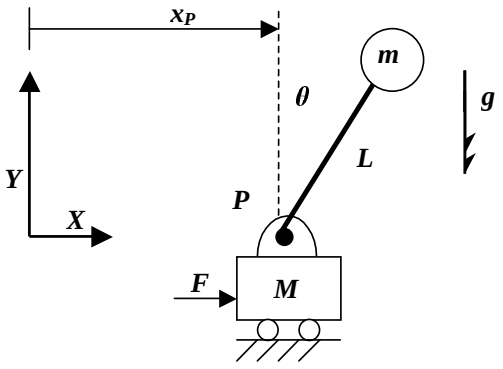

Figure 2-1: The classic inverted pendulum on a cart system.

2.1.1 Dynamic Model of Classic Inverted Pendulum

The results of the linearized dynamic model are briefly given here for later comparison with the arcing base inverted pendulum. The dynamics of the pendulum can be determined by first applying the principle of angular momentum about the moving pivot, P, which yields

$$mL^2\ddot{\theta} + mL\ddot{x}_P = mgL\theta - b\dot{\theta} \tag{2.1}$$

where b is the viscous damping in the pivot P and g represents gravity.

Applying a force balance around the base of the cart yields a second dynamic equation governing the cart motion. Combining these results one may obtain the following description of the system in state determined form, with the state vector, $\vec{x}$, where

$$\vec{\mathbf{x}}^T = \begin{bmatrix} x_P & \dot{x}_P & \theta & \dot{\theta} \end{bmatrix} \tag{2.2}$$

and

$$\dot{\vec{\mathbf{x}}} = \begin{bmatrix} 0 & 1 & 0 & 0 \\ 0 & \frac{-c}{M} & \frac{-mg}{M} & \frac{b}{ML} \\ 0 & 0 & 0 & 1 \\ 0 & \frac{c}{ML} & \frac{g(M+m)}{ML} & \frac{-b(M+m)}{mML^2} \end{bmatrix} \vec{\mathbf{x}} + \begin{bmatrix} 0 \\ \frac{1}{M} \\ 0 \\ \frac{-1}{ML} \end{bmatrix} F \tag{2.3}$$

where c is the viscous friction on the cart base.

These dynamic results are used in the implementation of common control schemes for the inverted pendulum problem.

2.1.2 Common Control Approaches

Common approaches to stabilizing this system include full state feedback and root locus techniques. Control schemes such as the one presented in Ogata's *Modern Control Engineering* [2] implement full state feedback using the state space representation of the system presented in equations(2.2) and (2.3) above.

A second common approach, covered in MIT's 6.302, is to use root locus techniques

applied to just the pendulum. From equation (2.1), the transfer function governing motion for the pendulum becomes

$$\frac{\Theta(s)}{X_P(s)} = \frac{-mLs^2}{mL^2s^2 + bs - mgL} \tag{2.4}$$

This system is unstable, (with $b = 0$ the open loop poles are at $s = \pm\sqrt{\frac{g}{L}}$).

The important difference between these approaches is that in the first we control the input force, F, and in the second we control position, x_P.

2.2 Inverted Pendulum with Arcing Base

The physical system examined here differs significantly from the classic inverted pendulum, because the base no longer travels in a linear motion. The pendulum was mounted to a motor with its axis of rotation parallel to the ground. As a result the base of the pendulum now travels in an arc in the xy plane. This is shown in Figure 2-2, where the base of the pendulum rotates at a radius R about the fixed point Q (representing the axis of the motor). The system is now fully determined by the coordinates θ and α, where θ measures the pendulum angle with respect to the ground as before and α measures the angle of the base of the pendulum. Figure 2-2.b identifies the coordinates of the pivot P and the angle β, which measures the angle of the pendulum relative to the base of the pendulum. The input to the system is now the torque, T, applied by the motor.

2.3 Equations of Motion for Arcing Base Inverted Pendulum

Let x_P and y_P denote the coordinates of the pivot, P, as shown in Figure 2-2.b. The equations of motion describing the base of the pendulum are obtained by first determining x_P and y_P as a function of α and then taking consecutive derivatives to

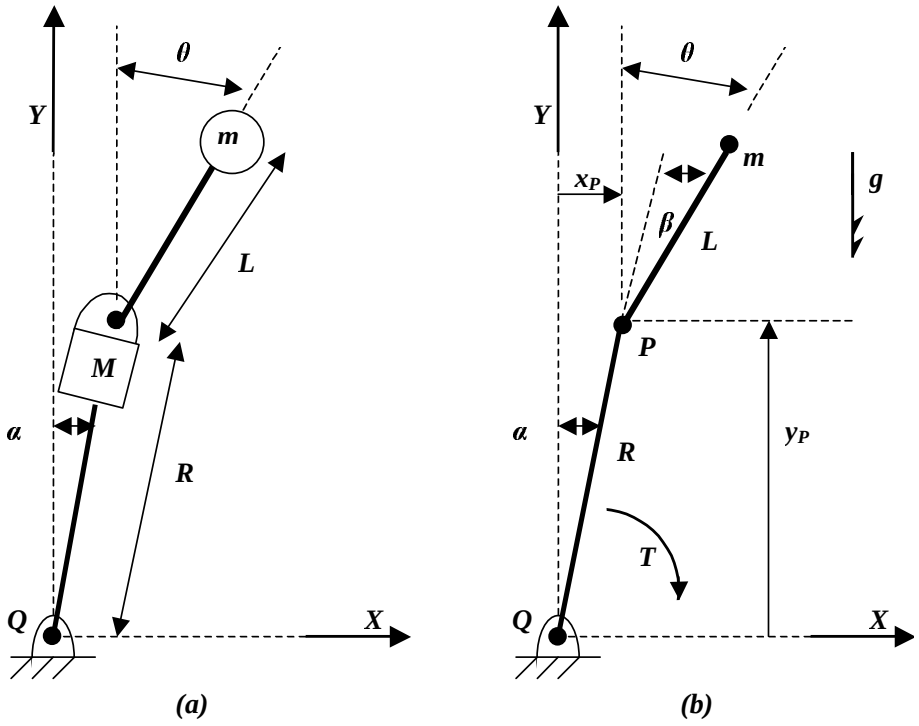

Figure 2-2: The inverted pendulum with pivot, P, travelling in an arc about Q.

obtain the velocity and acceleration of P.

$$x_P = R\sin(\alpha) \tag{2.5}$$

$$y_P = R\cos(\alpha) \tag{2.6}$$

$$\dot{x}_P = R\cos(\alpha)\dot{\alpha} \tag{2.7}$$

$$\dot{y}_P = -R\sin(\alpha)\dot{\alpha} \tag{2.8}$$

$$\ddot{x}_P = -R\sin(\alpha)\dot{\alpha}^2 + R\cos(\alpha)\ddot{\alpha} \tag{2.9}$$

$$\ddot{y}_P = -R\cos(\alpha)\dot{\alpha}^2 - R\sin(\alpha)\ddot{\alpha} \tag{2.10}$$

Similarly, the equations of motion of the mass, m, can be given in terms of θ and the position of P

$$x = x_P + L\sin(\theta) \tag{2.11}$$

$$y = y_P + L\cos(\theta) \tag{2.12}$$

$$\dot{x} = \dot{x}_P + L\cos(\theta)\dot{\theta} \tag{2.13}$$

$$\dot{y} = \dot{y}_P - L\sin(\theta)\dot{\theta} \tag{2.14}$$

$$\ddot{x} = \ddot{x}_P - L\sin(\theta)\dot{\theta}^2 + L\cos(\theta)\ddot{\theta} \tag{2.15}$$

$$\ddot{y} = \ddot{y}_P - L\cos(\theta)\dot{\theta}^2 - L\sin(\theta)\ddot{\theta} \tag{2.16}$$

The position of the P relative to the origin at Q, is given in vector form by $\vec{q}$

$$\vec{q} = x_P\hat{e}_x + y_P\hat{e}_y \tag{2.17}$$

The position of the mass m with respect to the pivot, P, is given by $\vec{r}$

$$\vec{r} = L\sin(\theta)\hat{e}_x + L\cos(\theta)\hat{e}_y \tag{2.18}$$

The velocities of the pivot, P, and of the mass, m, are given by $\vec{v}_P$ and $\vec{v}$, respectively

$$\vec{v}_P = \dot{x}_P\hat{e}_x + \dot{y}_P\hat{e}_y \tag{2.19}$$

$$\vec{v} = \dot{x}\hat{e}_x + \dot{y}\hat{e}_y \tag{2.20}$$

Having determined the equations of motion for the system we will now model the dynamic response of the pendulum.

2.4 Dynamic Model of Pendulum with Arcing Base

The dynamic model of the system is obtained by first determining the dynamics of the pendulum, using the principle of angular momentum, and the dynamics of the base, using a torque balance around Q. These results are then combined for the compelete system model.

2.4.1 Dynamics of the Pendulum

The first step to determining the dynamic model is to apply the angular momentum principle about the moving point P. The principle of angular momentum states

$$\frac{d\vec{H}_P}{dt} + \vec{v}_P \times \vec{p} = \sum \vec{\tau}_{ext} \tag{2.21}$$

where $\vec{H}_P$ is the angular momentum about P, $\vec{p}$ is the linear momentum of m, and $\vec{\tau}_{ext}$ are the external torques about P.

Remembering that $\vec{p} = m\vec{v}$, the angular momentum about P is given by

$$\begin{aligned}
\vec{H}_P &= \vec{r} \times \vec{p} && (2.22)\\
&= [L\sin(\theta)\hat{e}_x + L\cos(\theta)\hat{e}_y] \times m[\dot{x}\hat{e}_x + \dot{y}\hat{e}_y] && (2.23)\\
&= m[L\sin(\theta)\dot{y} - L\cos(\theta)\dot{x}]\hat{e}_z && (2.24)
\end{aligned}$$

Substituting the equations of motion for $\dot{x}$ and $\dot{y}$ determined in Section 2.3, we have

$$\begin{aligned}
\vec{H}_P = m[&L\sin(\theta)(-R\sin(\alpha)\dot{\alpha} - L\sin(\theta)\dot{\theta})\\
&-L\cos(\theta)(R\cos(\alpha)\dot{\alpha} + L\cos(\theta)\dot{\theta})]\hat{e}_z && (2.25)\\
= -mL[&R(\sin(\alpha)\sin(\theta) + \cos(\theta)\cos(\alpha))\dot{\alpha} + L(\sin^2(\theta) + \cos^2(\theta))\dot{\theta}]\hat{e}_z && (2.26)
\end{aligned}$$

Using the trigonometric identities $\sin^2(\theta)+\cos^2(\theta) = 1$ and $\cos(\theta-\alpha) = \cos(\theta)\cos(\alpha)+\sin(\theta)\sin(\alpha)$ the equation above becomes

$$\vec{H}_P = -mL[R\cos(\theta - \alpha)\dot{\alpha} + L\dot{\theta}]\hat{e}_z \tag{2.27}$$

Taking the derivative to obtain the first term of equation (2.21) we have

$$\frac{d\vec{H}_P}{dt} = -mL[-R\sin(\theta-\alpha)(\dot{\theta}-\dot{\alpha})\dot{\alpha} + R\cos(\theta-\alpha)\ddot{\alpha} + L\ddot{\theta}]\hat{e}_z \tag{2.28}$$

Calculating the second term in the angular momentum equation (2.21) we have

$$\vec{v}_P \times \vec{p} = [\dot{x}_P\hat{e}_x + \dot{y}_P\hat{e}_y] \times m[\dot{x}\hat{e}_x + \dot{y}\hat{e}_y] \tag{2.29}$$

$$= m[\dot{x}_P\dot{y} - \dot{y}_P\dot{x}]\hat{e}_z \tag{2.30}$$

Substituting again from the equations of motion in Section 2.3 and using the trigonometric identity $\sin(\theta-\alpha) = (\cos(\alpha)\sin(\theta) - \sin(\alpha)\cos(\theta))$ we obtain

$$\vec{v}_P \times \vec{p} = -mRL\sin(\theta-\alpha)\dot{\theta}\dot{\alpha}\hat{e}_z \tag{2.31}$$

The external torques about P are due to friction in the pivot joint and gravity on the pendulum mass, m. So the right hand side of equation (2.21) yields

$$\sum \vec{\tau}_{ext} = \vec{\tau}_f + \vec{\tau}_g \tag{2.32}$$

where $\vec{\tau}_f$ is the torque due to friction and $\vec{\tau}_g$ is the torque due to gravity. By inspection the viscous friction torque is

$$\vec{\tau}_f = b\dot{\beta}\hat{e}_z \tag{2.33}$$

where we have defined positive torque in the $-\hat{e}_z$ direction. Since $\beta = \theta - \alpha$,

$$\vec{\tau}_f = b(\dot{\theta}-\dot{\alpha})\hat{e}_z \tag{2.34}$$

Again, it is important to note here that $\hat{e}_z$ is positive in the $-\alpha$ direction, which explains the positive sign on this damping term.

The force due to gravity on the pendulum mass is given by $\vec{f}_g = -mg\hat{e}_y$. Thus,

the torque due to gravity is

$$\vec{\tau}_g = \vec{r} \times \vec{f}_g \tag{2.35}$$

$$= [L\sin(\theta)\hat{e}_x + L\cos(\theta)\hat{e}_y] \times [-mg\hat{e}_y] \tag{2.36}$$

$$= -mgL\sin(\theta)\hat{e}_z \tag{2.37}$$

Summing equations (2.34) and (2.37), equation (2.32) yields

$$\sum \vec{\tau}_{ext} = [-mgL\sin(\theta) + b(\dot{\theta} - \dot{\alpha})]\hat{e}_z \tag{2.38}$$

Now substituting equations (2.28), (2.31), and (2.38) into the angular momentum equation (2.21) and simplifying, we have the non-linear dynamic model of the pendulum.

$$mLR\sin(\theta - \alpha)\dot{\alpha}^2 + mLR\cos(\theta - \alpha)\ddot{\alpha} + mL^2\ddot{\theta} = mgL\sin(\theta) - b(\dot{\theta} - \dot{\alpha}) \tag{2.39}$$

Linearizing about $\theta \approx 0$ and $\alpha \approx 0$ we obtain the following small angle approximations:

$$\sin(\theta) \approx \theta$$

$$\cos(\theta) \approx 1$$

$$\sin(\theta - \alpha) \approx \theta - \alpha$$

$$\cos(\theta - \alpha) \approx 1$$

$$\dot{\theta}^2, \dot{\alpha}^2, \dot{\theta}\dot{\alpha} \approx 0$$

Linearizing equation (2.39) we obtain the following linear approximation of the pendulum dynamics near the unstable equilibrium:

$$mLR\ddot{\alpha} + mL^2\ddot{\theta} = mgL\theta - b(\dot{\theta} - \dot{\alpha}) \tag{2.40}$$

which can be rewritten as

$$\ddot{\theta} = \frac{mgL\theta - b(\dot{\theta} - \dot{\alpha}) - mLR\ddot{\alpha}}{mL^2} \tag{2.41}$$

or

$$\ddot{\alpha} = \frac{mgL\theta - b(\dot{\theta} - \dot{\alpha}) - mL^2\ddot{\theta}}{mLR} \tag{2.42}$$

Thus, we have obtained a linearized model of the pendulum's motion.

2.4.2 Dynamics of the Base

To complete the model of the system we now look at the motion of the base of the pendulum. In order to determine the dynamic response we take a torque balance about the point Q. (Here we define torque to be positive in the positive α direction or clockwise in the view of Figure 2-2.)

The total inertia of the base, with the pendulum attached, becomes $I + MR^2$, where I is the motor inertia, M is the mass of the base of the pendulum, and R is the distance from the motor axis, Q, to the pendulum pivot, P. A torque balance around Q yields

$$\sum \vec{\tau} = (I + MR^2)\ddot{\alpha} \tag{2.43}$$

The sum of the torques about Q is given by

$$\sum \vec{\tau} = \vec{T} + \vec{\tau}_f + \vec{\tau}_{pend} + \vec{\tau}_g \tag{2.44}$$

where $\vec{T}$ is the torque applied to the system by the motor, $\vec{\tau}_f$ is the frictional damping in the motor, $\vec{\tau}_{pend}$ is the torque due to the pendulum force, $\vec{f}_{pend}$, and $\vec{\tau}_g$ is the torque due to gravity on the base of the pendulum mass, M.

In order to determine $\vec{f}_{pend}$, the force the pendulum exerts on the base, we use a force balance on the pendulum mass, m. The free body diagram is shown in Figure 2-3. Summing forces in the x and y directions on the pendulum mass, m, in Figure

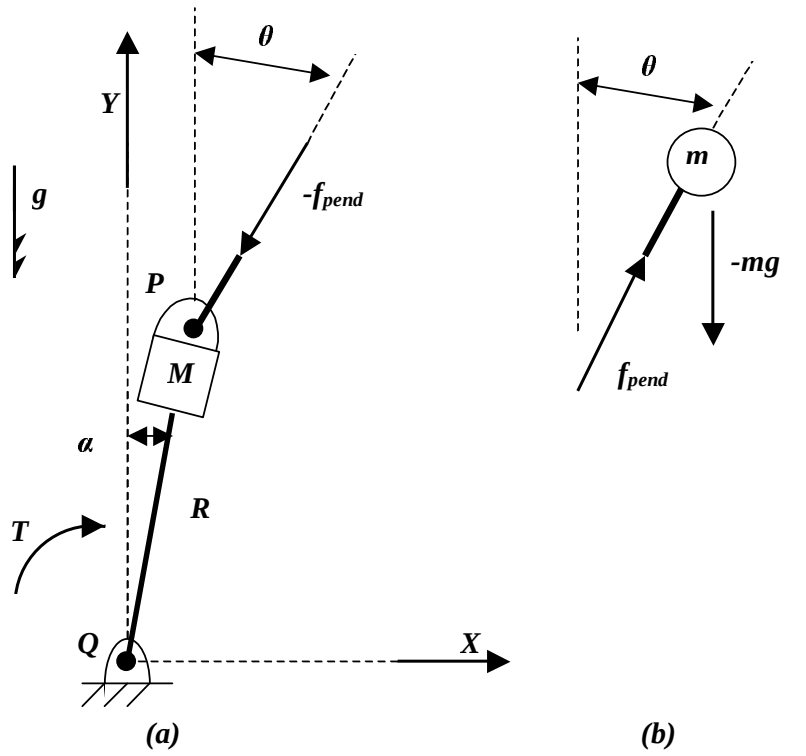

Figure 2-3: Free Body Diagram of m. *(a)* The base of the pendulum with pendulum force. *(b)* The mass, m.

2-3.b, we have

$$\vec{f}_{pend}\sin(\theta) = m\ddot{x} \tag{2.45}$$

$$\vec{f}_{pend}\cos(\theta) - mg = m\ddot{y} \tag{2.46}$$

where $\vec{f}_{pend}$ is the force in the pendulum shaft. From this we obtain

$$\vec{f}_{pend} = m[\ddot{x}\hat{e}_x + (\ddot{y} + g)\hat{e}_y] \tag{2.47}$$

The torque the pendulum exerts on the base is then

$$\vec{\tau}_{pend} = \vec{q} \times -\vec{f}_{pend} \tag{2.48}$$

$$= [x_P\hat{e}_x + y_P\hat{e}_y] \times -m[\ddot{x}\hat{e}_x + (\ddot{y} + g)\hat{e}_y] \tag{2.49}$$

$$= -m[x_P(\ddot{y} + g) - y_P\ddot{x}]\hat{e}_z \tag{2.50}$$

Substituting the appropriate equations of motion from Section 2.3, applying the trigonometric identities used previously, and linearizing, we obtain

$$\vec{\tau}_{pend} = m[R^2\ddot{\alpha} + RL\ddot{\theta} - gR\alpha]\hat{e}_z \tag{2.51}$$

Gravity acting on the base of the pendulum produces a force, $\vec{F}_g = -Mg\hat{e}_y$, the resulting torque on the motor is

$$\vec{\tau}_g = \vec{q} \times \vec{F}_g \tag{2.52}$$

$$= [x_P\hat{e}_x + y_P\hat{e}_y] \times [-Mg\hat{e}_y] \tag{2.53}$$

$$= -Mgx_P\hat{e}_z \tag{2.54}$$

After substitution from equation (2.5),

$$\vec{\tau}_g = -RMg\sin(\alpha)\hat{e}_z \tag{2.55}$$

Note that since we have defined positive torque to be opposite of $\hat{e}_z$ it will be necessary to invert $\vec{\tau}_g$ and $\vec{\tau}_{pend}$ for use in equation (2.44).

The frictional damping torque, $\vec{\tau}_f$, can be determined by inspection and is made positive in the direction of positive α

$$\vec{\tau}_f = -c\dot{\alpha} \tag{2.56}$$

Correcting the signs of each term to make torque positive in the direction of positive α and substituting (2.51), (2.55) and (2.56) into equation (2.44) we obtain the second equation of motion. The linearized result is

$$[(M+m)R^2 + I]\ddot{\alpha} = T - c\dot{\alpha} - mLR\ddot{\theta} + (M+m)gR\alpha \tag{2.57}$$

2.5 Dynamics for Combined Pendulum and Cart System

The dynamics of the combined system can found using equations (2.41) and (2.42) to alternately eliminate $\ddot{\theta}$ and $\ddot{\alpha}$ from equation (2.57). From this we obtain the following expressions:

$$\ddot{\alpha} = \frac{T + MgR\alpha - c\dot{\alpha} - mgR(\theta - \alpha) + \frac{bR}{L}(\dot{\theta} - \dot{\alpha})}{MR^2 + I} \tag{2.58}$$

and

$$\ddot{\theta} = \frac{-TR + gI\theta + cR\dot{\alpha} + g[(M+m)R^2](\theta - \alpha) - \frac{b}{mL}[(M+m)R^2 + I)(\dot{\theta} - \dot{\alpha})}{L(MR^2 + I)} \tag{2.59}$$

2.5.1 Change of Coordinates to α and β

The measurable coordinates in the simplest implementation of this system are α and β, where α is the angle of the base, and β is the angle of the pendulum with respect to the base such that $\beta = \theta - \alpha$, as shown in Figure 2-2. Thus, since we will measure β with a simple potentiometer, it is advantageous to rewrite the system in the α and β coordinate system.

Substituting $\beta = \theta - \alpha$ into equation (2.58), we have

$$\ddot{\alpha} = \frac{T + MgR\alpha - c\dot{\alpha} - mgR\beta + \frac{bR}{L}\dot{\beta}}{MR^2 + I} \tag{2.60}$$

Now adding and subtracting the term $gI\alpha$ from equation (2.59) and grouping the $\theta - \alpha$ term we have

$$\ddot{\theta} = \frac{-TR + gI\alpha + cR\dot{\alpha} + g[(M+m)R^2 + I](\theta - \alpha) - \frac{b}{mL}[(M+m)R^2 + I)(\dot{\theta} - \dot{\alpha})}{L(MR^2 + I)} \tag{2.61}$$

Substituting $\beta = \theta - \alpha$ this becomes

$$\ddot{\theta} = \frac{-TR + gI\alpha + cR\dot{\alpha} + g[(M+m)R^2 + I]\beta - \frac{b}{mL}[(M+m)R^2 + I)\dot{\beta}}{L(MR^2 + I)} \tag{2.62}$$

Calculating $\ddot{\beta}$ we have

$$\begin{aligned}\ddot{\beta} &= \ddot{\theta} - \ddot{\alpha} \\ &= \frac{-T(R+L) + g(I - MRL)\alpha + c(R+L)\dot{\alpha}}{L(MR^2 + I)} \\ &\quad + \frac{g[(M+m)R^2 + I + mRL]\beta - b[\frac{(M+m)R^2+I}{mL} + R]\dot{\beta}}{L(MR^2 + I)}\end{aligned} \tag{2.63}$$

2.6 Results in State Determined Form

This system can now be written in state-determined form

$$\dot{\vec{\mathbf{x}}} = \mathbf{A}\vec{\mathbf{x}} + \mathbf{B}u \tag{2.64}$$

where the input u is simply the applied torque, T, and the state vector, $\vec{\mathbf{x}}$ is given by

$$\vec{\mathbf{x}}^T = \begin{bmatrix} \alpha & \dot{\alpha} & \beta & \dot{\beta} \end{bmatrix} \tag{2.65}$$

The $\mathbf{A}$ and $\mathbf{B}$ matrices are determined directly from equations (2.60) and (2.63)

$$\mathbf{A} = \begin{bmatrix} 0 & 1 & 0 & 0 \\ \frac{MgR}{MR^2+I} & \frac{-c}{MR^2+I} & \frac{-mgR}{MR^2+I} & \frac{bR}{L(MR^2+I)} \\ 0 & 0 & 0 & 1 \\ \frac{g(I-MRL)}{L(MR^2+I)} & \frac{c(R+L)}{L(MR^2+I)} & \frac{g[(M+m)R^2+I+mLR]}{L(MR^2+I)} & \frac{-b[\frac{(M+m)R^2+I}{mL}+R]}{L(MR^2+I)} \end{bmatrix} \tag{2.66}$$

$$\mathbf{B}^T = \begin{bmatrix} 0 & \frac{1}{MR^2+I} & 0 & \frac{-(R+L)}{L(MR^2+I)} \end{bmatrix} \tag{2.67}$$

This solution lacks the simple elegance of the classic inverted pendulum on a cart system given in Section 2.1. However, the basic form is the same, with the addition

of two terms dependent on α. The first term quantifies the contribution to $\ddot{\alpha}$ resulting from gravity on the base of the pendulum ($\vec{\tau}_g \propto MgR\alpha$). The dependence of $\ddot{\beta}$ on α, however, is purely an artifact of the change of coordinates performed in section 2.5.1. Regardless of these differences, the design approach by full state feedback is essentially unchanged.

Chapter 3

MATLAB Model of the Inverted Pendulum

In analyzing the inverted pendulum problem, heavy use was made of MATLAB to model the system and examine the effects of various inputs and changes to the model. The following details the full state feedback approach employed here and the Simulink model used to analyze the system.

3.1 Theory of state feedback

The idea behind full state feedback is to make the feedback signal, u, dependent on the state of the system: $u = -\mathbf{K}\vec{\mathbf{x}}$, as shown in Figure 3-1. Thus our state equation, $\dot{\vec{\mathbf{x}}} = \mathbf{A}\vec{\mathbf{x}} + \mathbf{B}\mathbf{u}$, becomes

$$\dot{\vec{\mathbf{x}}} = (\mathbf{A} - \mathbf{B}\mathbf{K})\vec{\mathbf{x}} \tag{3.1}$$

Since the characteristic polynomial of this system is

$$|s\mathbf{I} - \mathbf{A} + \mathbf{B}\mathbf{K}| = (s + p_1)(s + p_2)\dots(s + p_n) \tag{3.2}$$

it is possible to place the poles of the system $(p_1, \dots, p_n)$ at a desired location with an appropriate choice of $\mathbf{K}$, provided that the system is completely state controllable and that all the states are available for feedback. For more information on the theory

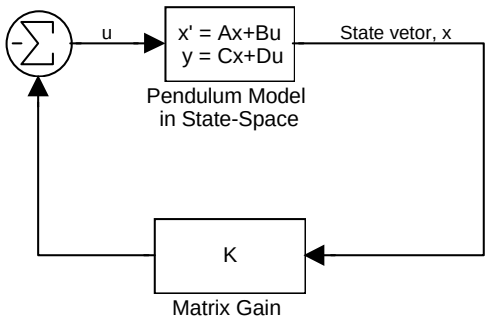

Figure 3-1: Basic State Feedback

of state feedback see *Modern Control Engineering* by Ogata [2].

Ackermann's formula for pole placement was used to place the closed loop poles at $-2 \pm 1.5i, -10$, and -10, given the linearized $\mathbf{A}$ and $\mathbf{B}$ matrices from Section 2.6. For details of this procedure see Appendix B.2.

3.2 Simulink Model

Figure 3-2 shows the Simulink model with the additional blocks required to plot the response of the system. The input and output blocks shown in the figure and discussed below are borrowed from the MATLAB file `penddemo.m`. The detailed system model with sensor gains is given in Figure 3-5.

3.2.1 Input

Since the model has no natural disturbances, it was necessary to create input disturbances to observe the system response. In Figure 3-2 there is an offset, α_{ref}, subtracted from α. Since full state feedback systems are regulator systems, meaning that they regulate to the origin of state space, this offset allows us to observe the step response of the system as follows.

In this system the origin of state space is $\alpha = \dot{\alpha} = \beta = \dot{\beta} = 0$, when the pendulum is balanced vertically and stationary. The offset has the effect of shifting the origin

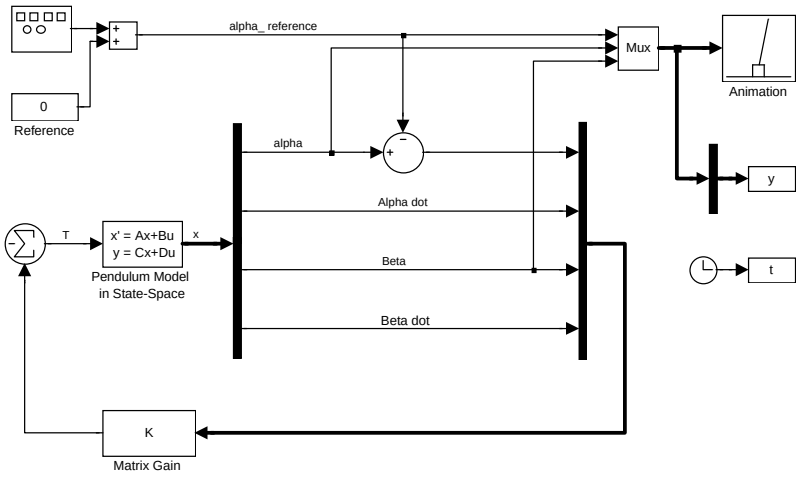

Figure 3-2: Simulink Model of Full State Feedback with the MATLAB's pendulum animation output and output to file.

of state space. We denote shifted coordinates with a $'$ symbol.

$$\alpha' = \alpha - \alpha_{ref} \tag{3.3}$$

and

$$\begin{aligned} \beta' &= \theta - \alpha' && (3.4)\\ &= \theta - (\alpha - \alpha_{ref}) && (3.5)\\ &= (\theta - \alpha) + \alpha_{ref} && (3.6)\\ &= \beta + \alpha_{ref} && (3.7) \end{aligned}$$

Since the reference offset is a constant it has no effect on the derivatives of α and β. Thus, the new origin of state space becomes

$$\alpha - \alpha_{ref} = \dot{\alpha} = \beta + \alpha_{ref} = \dot{\beta} = 0 \tag{3.8}$$

The origin of state space now corresponds to α and β non-zero, but equal and opposite. Fortunately, this condition also corresponds to a vertical pendulum ($\theta = 0$). Thus, the introduction of this offset simply has the effect of stabilizing the pendulum at non-

zero α. A square wave offset supplied to α by the function generator in the upper left of Figure 3-2, thus allows observation of the step response of the pendulum.

3.2.2 Output

The output blocks in Figure 3-2 include MATLAB's graphical pendulum animation and output to the workspace stored in the vector y.

Figure 3-3 graphically shows the pendulum balanced at non-zero α. The output shown here has been slightly modified from MATLAB's animation program `pendan.m` to show the pendulum with the rotary base. For the modified code see Appendix B.5.

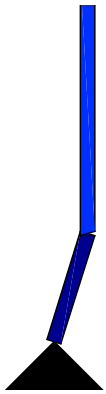

Figure 3-3: Modified MATLAB Pendulum Animation with pendulum balanced upright at non-zero α.

For a more detailed analysis, Figure 3-4 plots the data output from Simulink in the vector y, illustrating the response of the pendulum to a square wave offset in α.

It is apparent at steady state in Figure 3-4, that β is equal and opposite to α, indicating that the pendulum is standing upright. The lower half of the plot shows that θ is in fact equal to zero in the steady state.

It is worth note that, with damping equal to zero, as in the plots here, the values of the gain matrix, $\mathbf{K}$, are all negative. This means that with the feedback equal to $-\mathbf{K}\vec{\mathbf{x}}$ the control system is actually implementing positive feedback on all of the states. Although this may seem surprising, it is correct. Consider the classic inverted

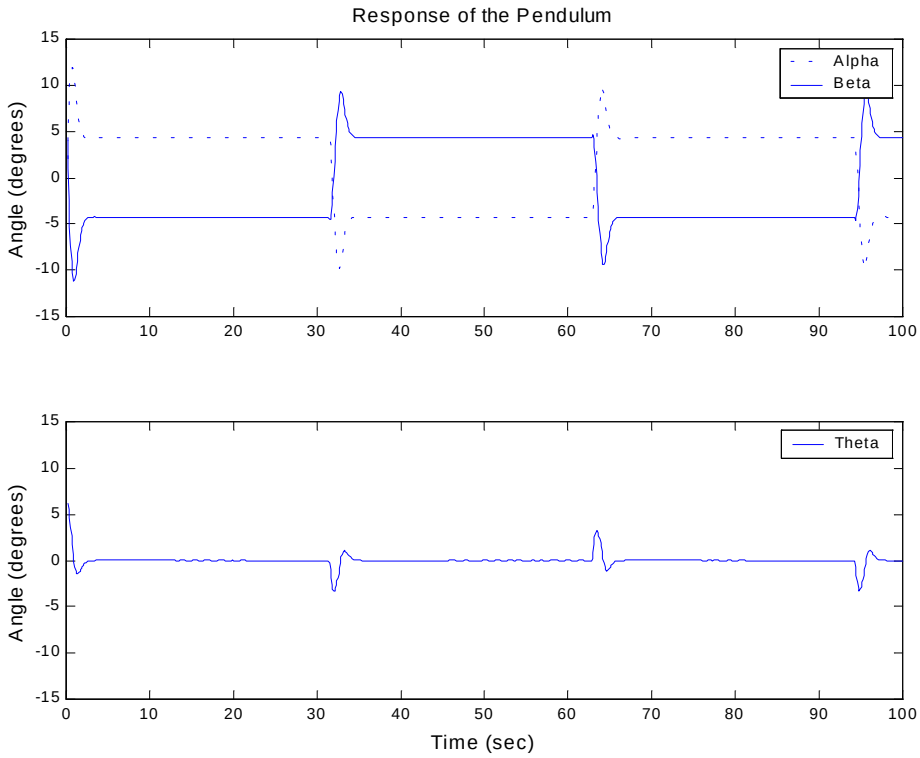

Figure 3-4: The modelled pendulum response to square wave reference input.

pendulum on a cart with the pendulum balanced at $x > 0$ and $\dot{x} = \theta = \dot{\theta} = 0$. Positive feedback indicates the system will initially respond by moving the cart in the $+x$ direction. This will cause the pendulum to lean back towards the origin with θ negative. Because the gains on the θ feedback are much higher than on x, this will cause the pendulum to correct by moving back towards $x = 0$. Thus, positive feedback actually gives the desired response.

Looking at Figure 3-4 you can see that the pendulum does respond to the step input by initially making deviations in α worse, causing θ to tilt in the direction of the desired equilibrium.

3.2.3 Detailed System Model

Having established the basic system and stability, the next step is to model the physical system. Figure 3-5 shows the model of the complete system, including the gains

of all the sensors and components discussed in Chapter 4. For simplicity the output is not shown. The gain matrix $\mathbf{K}_{sys}$ in the figure was determined by appropriately factoring out the system gains from the $\mathbf{K}$ matrix previously found using Ackermann's Formula. More detail on this adjustment is available in Appendix B.3.

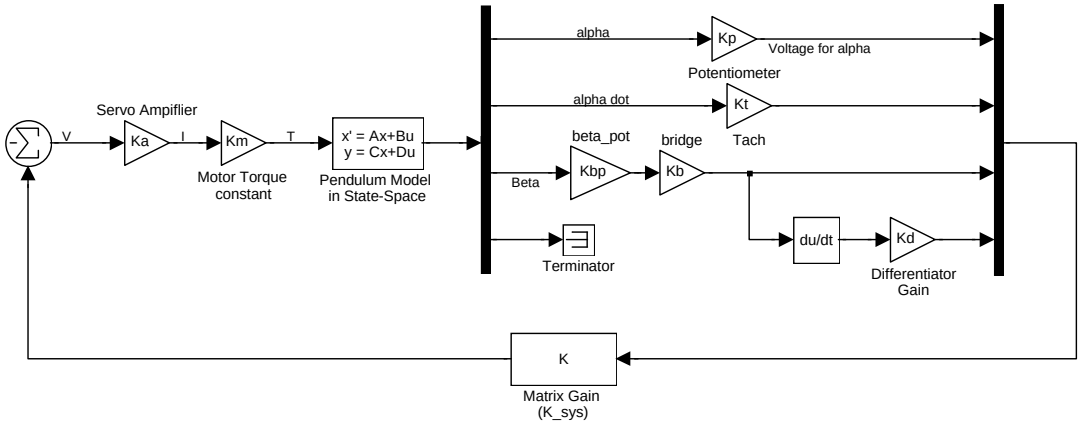

Figure 3-5: State Feedback with the system gains added to the model

This specific system was used to model the effects of noise on various inputs, non-linearities in the motor and general robustness to various conditions.

Chapter 4

Apparatus

4.1 2.010 Lab Platform

The inverted pendulum analyzed here was built on the MIT 2.010 undergraduate motor control lab platform. The 2.010 lab features an Aerotech 1135DC servo motor, mounted with its axis of rotation parallel to the ground and an aluminum inertia attached to the output shaft, as illustrated in Figure 4-1. The motor has a built-in tachometer and a potentiometer attached. Thus, velocity and position feedback for the motor were provided. An Aerotech 4020-LS linear power amplifier was used as a voltage controlled current source to power the motor. The relevant physical constants and gains for this system, given in Table 4.1, were determined by Adiel Smith and Ziaieh Sobhani in 2001 [3].

Table 4.1: Gains for the 2.010 Lab setup

Servo Amplifier Gain, K_a	1.9368	A/V
Motor Torque Constant, K_m	0.1697	Nm/A
Load Inertia, J	9.94×10^4	kg/m^2
Coulomb Friction Coefficient, K_f	0.0306	kgm^2/sec
Tachometer Gain Constant, K_t	0.0286	V/(rad/sec)
Potentiometer Gain Constant, K_p	0.2504	V/rad

4.2 Pendulum Constructed

The pendulum base was clamped to the motor inertia in the orientation shown in Figure 4-1. The pendulum was rigidly attached to the $\frac{1}{4}$" shaft passing through P. To measure the pendulum angle, β, a Bourns 6639S-1-103 precision potentiometer was attached to this shaft via a flexible coupling and supported from below.

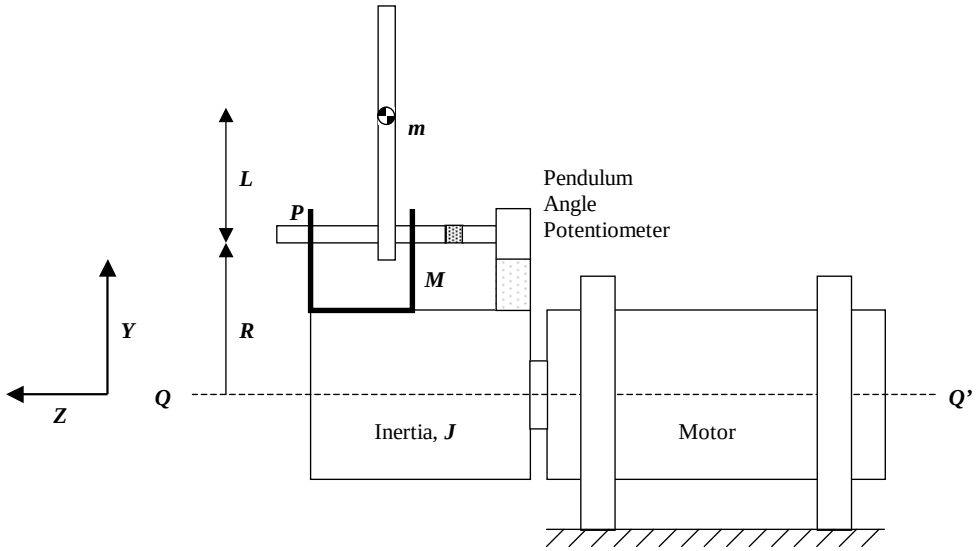

Figure 4-1: Side view of the inverted pendulum setup. The base of the pendulum was mounted on the inertia of a 2.010 lab motor.

The dimensions of the pendulum constructed are given in Table 4.2. The total inertia, I, includes the aluminum inertia, J, and the inertia of the clamp for mounting the pendulum base.

Table 4.2: Dimensions of the Pendulum Constructed

Radius of the arcing base, R	0.0725	m
Distance from base to cg of pendulum, L	0.0532	m
Mass of the base, M	0.05338	kg
Total inertia, I	0.001293	kgm^2
Mass of pendulum, m	0.00636	kg

4.3 Circuitry Added

4.3.1 Motor Range Limiting and Shut-off

The physical design of this system requires that α be stabilized. If α were to exceed $\approx 90^\circ$ from vertical, the pendulum could strike the work bench and harm the motor or the pendulum. To prevent the possibility of this happening a safety circuit was designed to limit the range of the motor. The details of this circuit are given in Appendix A.1. It functions by grounding the output to the servo amplifier when α exceeds a specified range.

In addition to this feature, a toggle switch was provided as an emergency off switch to ground the output to the servo amplifier.

4.3.2 Angle Measurement

Additional circuitry was necessary to measure the angle of the pendulum with respect to the base, β, and to differentiate this signal to obtain the angular velocity of the pendulum, $\dot{\beta}$, required for full state feedback.

The β signal was obtained by placing the angle-measuring potentiometer in a wheatstone bridge, the details of which are in Appendix A.3. The $\dot{\beta}$ signal was obtained using an analog op-amp differentiation of the β signal. This circuit is discussed in Appendix A.4.

Additional system gains introduced by these circuits are given in Table 4.3.

Table 4.3: Gains Introduced by Sensor Circuits

Gain of the β pot, K_{bp}	0.014529	V/°
Gain of the bridge circuit, K_b	9.8147	V/V
Gain of differentiator, K_d	0.0105	V/V

4.3.3 Feedback

The feedback was accomplished by sending the four states $(\alpha, \dot{\alpha}, \beta, \dot{\beta})$ to a summing op-amp with gains determined by specific test conditions in the MATLAB model. It was convenient to use potentiometers on the feedback signals so that the gains could be quickly adjusted for different test conditions.

Chapter 5

Procedure

5.1 Setup

The first step in testing this control system is mounting the pendulum assembly to the motor inertia. It is critical that the pendulum be mounted such that the base of pendulum is at the peak of the arc when $\alpha = 0$. The position controller detailed in Appendix A.2 was used to hold the motor inertia steady in the correct position while mounting the pendulum.

After securing the pendulum we establish the $\beta = 0$ reference point. This was done by first balancing the pendulum upright and securing the pot such that the β signal was close to zero. The wheatstone bridge circuit discussed in Appendix A.3 was then adjusted to make $\beta = 0$ when the pendulum is balanced upright and $\alpha = 0$.

Finally, one should check that the motor-range-limiting circuit is functioning correctly (shutting off the motor when α exceeds $\approx 45^\circ$ from vertical) and that the signs of all the feedback signals are positive in the positive direction of the motor.

5.2 Testing and Debugging

The procedure attempted for stabilizing the physical system was largely one of testing and debugging. The MATLAB model was employed to determine the system gains as discussed in Chapter 3, based on the specific conditions being tested. The four

feedback resistors in the summer op-amp were adjusted and primarily qualitative observations were made of the system response. The most significant observation made during debugging was that damping was not negligible.

It was immediately observed that viscous friction in the pendulum joint introduced by the β pot assemblage was considerable. The pendulum was easy to stand upright, so easy, in fact, that it was difficult to precisely determine where $\beta = 0$ really was. Since the magnitude of the damping was not easy to measure, it was estimated by observing the system response with different levels of damping added to the model. By this method the value of b was estimated to be near 0.004 kgm^2/sec.

Regarding the motor, it was determined previously by Smith and Sobhani [3] that the primary friction was not viscous but coulomb in nature. This means that the viscous friction, c, in the dynamic model was essentially zero, while the coulomb friction in the motor was approximated as

$$T_f = -sign(\dot{\alpha})K_f \tag{5.1}$$

where the $sign(\dot{\alpha})$ term ensures that this effect always opposes the direction of motion of the motor. T_f here represents the constant torque that is consumed by the friction internal to the motor caused by gears and bearings. The Coulomb friction must be overcome before any torque will register on the output shaft.[1] This Coulomb friction effect is commonly known as a dead zone or dead band. The magnitude of K_f, given in Table 4.1, was found to be 0.0306 kgm^2/sec^2, which corresponds to T_f of 0.0306 Nm.

This dead band torque is larger than the peak torque of 0.0154 Nm required for the stabilization of the pendulum modelled in Figure 3-4. This result explains the lack of response observed in the physical system, since for moderate deviations the control signal was overwhelmed by the dead zone of the motor. To counteract this effect a circuit was designed to compensate for the dead zone by adding a corresponding voltage to "preload" the output signal to the motor. This circuit made it possible to

[1]The effects of stiction are not considered here.

observe the system response and enable further testing.

Following the initial compensation for the dead zone, it was observed that the system response was asymmetric, consistently overcorrecting in the negative direction and undercorrecting in the positive direction. This observation inspired a better attempt at measuring the dead zone by observing the minimum voltage required to make the motor turn. As expected, the values varied significantly depending on direction and other effects, which probably include temperature, recent use, and possibly even position of the motor.

It was difficult to measure the minimum voltage with accuracy or precision, however, the result was clearly asymmetric. The circuit discussed in Appendix A.5 was implemented to better compensate for the asymmetric dead zone, based on the best estimate of the size of the dead zone.

Unfortunately, even this better compensation failed to stabilize the system. Upon examination of the effects of the dead zone in the MATLAB model (to be discussed in Chapter 6), the attempt at stabilizing the inverted pendulum by the current method in the time available was abandoned.

Chapter 6

Results and Discussion

The results of these tests were inconclusive. In theory the inverted pendulum with the arcing base considered here is no more difficult to stabilize than the classic inverted pendulum on a cart. However, the practical problems in implementing the control system were considerable.

6.1 Damping

The effects of damping are believed to be the dominant cause of failure. Damping in the pendulum joint, introduced primarily by the β potentiometer and the flexible coupling joining it to the pendulum shaft, was significant. While this damping has a large impact on the model, stabilization is possible, provided the damping is accounted for. Damping in the pendulum joint hindered this investigation because the magnitude of the damping was hard to measure or even estimate. A robust stabilization would require eliminating this damping altogether or at least determining a better way to measure it.

The effect of coulomb friction in the motor is a more serious problem because the model has no way to compensate for this non-linearity. Examining the effect of the motor dead zone in the MATLAB model showed that the system was intolerant to even a small dead zone. In general, the simulated pendulum became oscillatory and unstable as the magnitude of the dead zone increased. Figures 6-1 and 6-2 illustrate

this trend. The simulated responses shown here model the pendulum constructed with an estimated damping of 0.004kgm^2/sec. These plots show the pendulum regulating to the origin, given an initial condition where it is balanced upright at $\alpha = 0.02$ rad ($\alpha \approx 1°$).

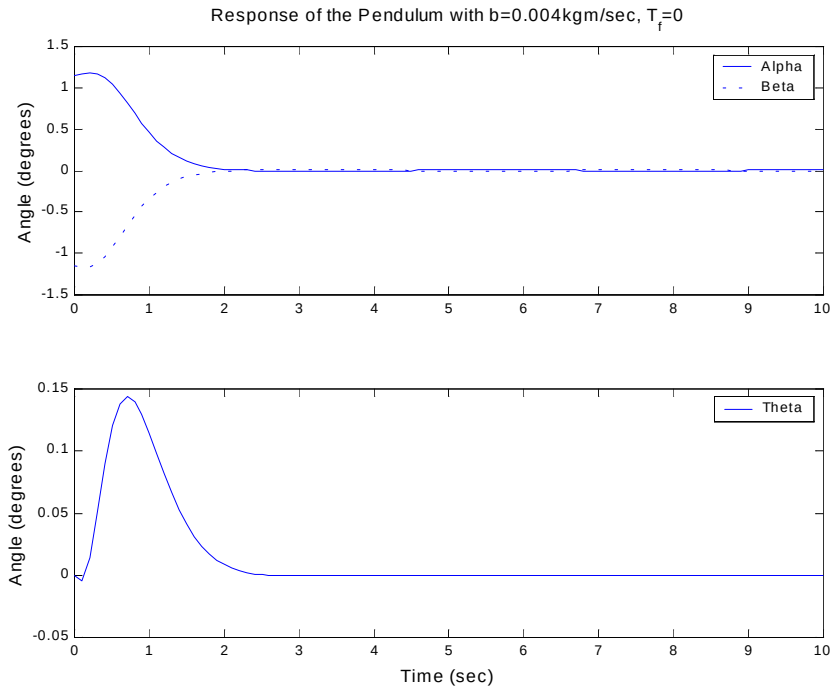

Figure 6-1: The simulated pendulum response to an initial condition. With no dead zone the system is stable.

Figure 6-1 illustrates the stable response with no dead zone ($T_f = 0$). Figure 6-2, however, illustrates how the system oscillates with increasing size of the dead zone. In Figure 6-2.a, the pendulum oscillates between $\alpha \approx \pm 2°$ with the dead zone modelled as 1% of the measured dead zone on the 2.010 motor ($T_f = 3.06 \times 10^{-4}$). Figure 6-2.b shows the oscillations increased to $\approx \pm 20°$ with a dead zone of 10% of the measured value ($T_f = 3.06 \times 10^{-3}$).

These oscillations quickly exceed the linear range of the model, indicating the system is actually unstable for even a relatively small dead zone. The magnitude of the oscillations was fairly independent of the initial condition given here; it increased

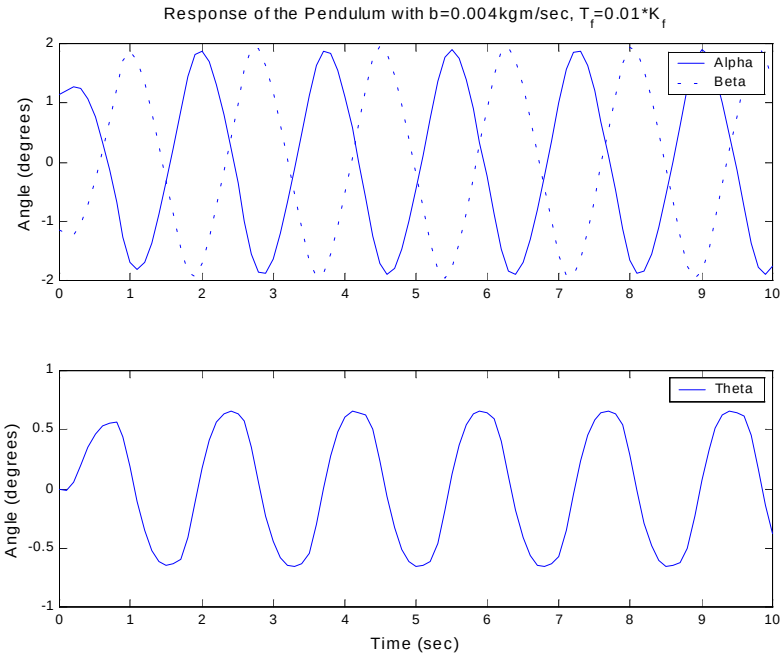

(a)

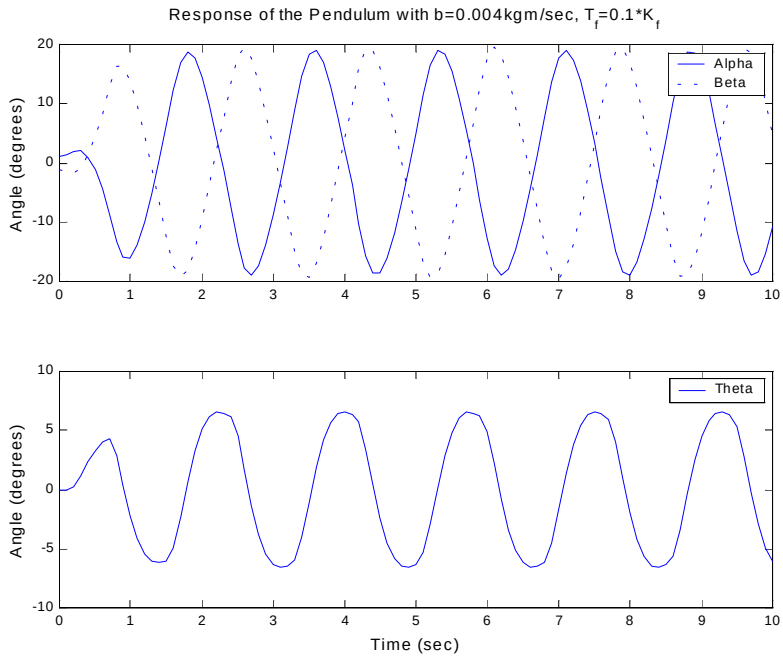

(b)

Figure 6-2: The pendulum oscillates with dead zone at *(a)* 1% and *(b)* 10% of estimated dead zone on the 2.010 motor.

moderately as the damping, b, increased and in general decreased as the pendulum size increased. Since our experimental measurements of the dead zone threshold were at best able to pinpoint the magnitude of the dead zone within 10%, stabilization of the current system using preloading method of dead zone compensation was deemed futile.

6.2 Recommendations

A general recommendation for future attempts at stabilization would be to make the pendulum larger and sturdier. During testing it was observed that some backlash developed in the mounting between the pendulum and the shaft to the β pot. While larger issues limited the success of this study, a sturdier construction would easily eliminate this problem and potential nonlinearities in the system. Due primarily to safety concerns the pendulum constructed was very small. As a result the linear range of motion for P was less than 7cm ($\approx$ 3in). While the dimensions of the pendulum have no impact on the ideal MATLAB model, the small pendulum made observation and debugging of the system difficult. Furthermore, a bigger, more massive pendulum would add robustness to unaccounted for damping. Since a larger plant would naturally require larger torques while the dead zone remains constant, the effects of the dead zone would be diminished.

Eliminating the dead zone altogether could be accomplished by one of two techniques. Conceptually the most straightforward would be to add a torque feedback loop around the motor. The result of the dead zone was that the output torque to the system was less than that specified by the controller. Placing feedback around the motor we could ensure the output torque matched the desired value. The difficulty in this approach would be to measure the torque output of the motor. Provided this torque could be measured, a torque feedback loop would be the simplest solution to eliminating the dead zone.

A second solution to the dead zone problem would be to modify the system model to control the position of the base rather than torque. From equation (2.40) the

transfer function for the pendulum only can be written as

$$\frac{\Theta(s)}{A(s)} = \frac{s(mLRs - b)}{-mL^2s^2 - bs + mgL} \tag{6.1}$$

This system can be stabilized using root locus techniques, similar to those commonly used with the classic linear inverted pendulum, as mentioned in section 2.1.2. Unfortunately, this approach involves considerable modifications to the control theory presented here.

Unfortunately, issues with damping and the dead zone hindered the true goal of this study, which was the stabilization of the inverted pendulum using simple analog components. Obtaining the $\dot{\beta}$ signal via an op-amp differentiator was an anticipated challenge for implementing full state feedback in this manner.

The analog differentiator employed here and discussed in detail in Appendix A.4 differed considerably from the theoretical response below frequencies of 1.5 Hz. Since these low frequencies are important in this system it may be worthwhile to improve the differentiator after the improvements listed above. This effect is not considered as great because the model seemed to be robust to a factor of 2 miscalculation in K_d, which should cover the difference for the relevant frequencies.

Appendix A

Circuits

A.1 Motor Range Limiting Circuit

The motivation behind this circuit was to limit the range of motion of the motor. Since the motor is physically restricted to $\approx 180°$ of motion when the pendulum assembly is mounted, it would be dangerous for the system to go unstable and have the pendulum strike the work bench. The following circuit causes the motor to shut off whenever the motor angle, α, exceeds a specified range—here $\approx 45°$ from vertical.

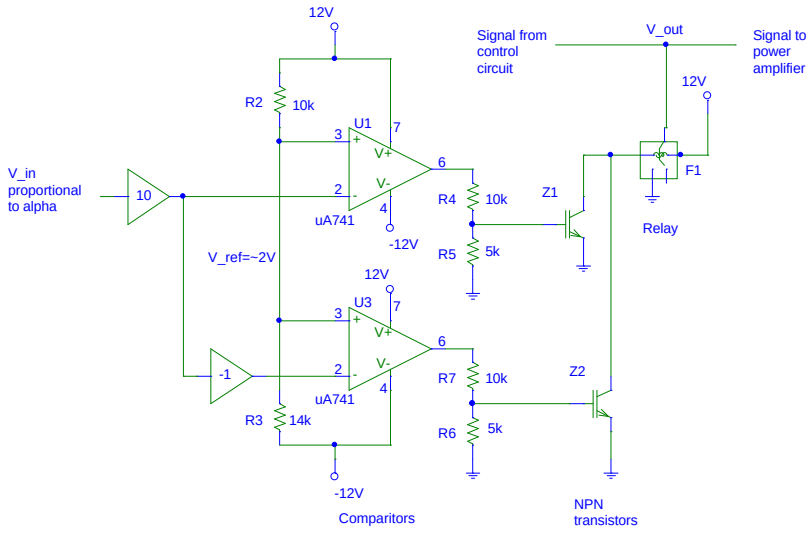

Figure A-1: This circuit limits the range of α to $\pm 45°$.

Consider first the top half of the circuit in Figure A-1. The motor position, α, was measured through a geared potentiometer with a gain of 0.2584 V/rad. Here this signal was further amplified by a factor of 10, to obtain a working voltage range of $\pm$4V, corresponding to the possible 180° of travel. The amplified input signal was compared to an adjustable reference voltage of $\approx$ 2V, which corresponds to an α of about 45° from vertical. When the amplified α input exceeds the reference voltage on the 741 Operational Amplifier, (that is, when α exceeds the specified limit), the output of the op amp will be high. This high output in turn activates an NPN transistor through the resistor divider shown. When the NPN transistor is active, current will flow through the relay, activating it and grounding the signal to the servo amplifier. Providing this 0V input to the servo amplifier turns off the motor. Thus, when α exceeds the set bound, the motor is turned off.

The lower half of this circuit performs the same operation on the inverted signal, thus the motor has been effectively restricted to a range with absolute value of 45°.

A.2 Motor Position Controller

It is critical for this system that the pendulum be mounted to the motor inertia such that the pendulum pivot, P, is directly above Q (at the top of the arc) when $\alpha = 0$. The motor position controller, shown in Figure A-2, is used to hold the motor at $\alpha = 0$ so that the pendulum can be mounted correctly. This controller has a very high gain and reacts quite forcefully when α is significantly different from zero. For this reason, it is recommended to only engage the position controller after manually aligning α to within $\pm$15° of zero.

A.3 Pendulum Angle, β, Measurement

To measure the angular position of the pendulum a Bourns 6639S-1-103 precision potentiometer was mounted on the shaft at the base of the pendulum with the flexible coupling shown in Figure 4-1. This potentiometer has a resistance of 10KΩ linear

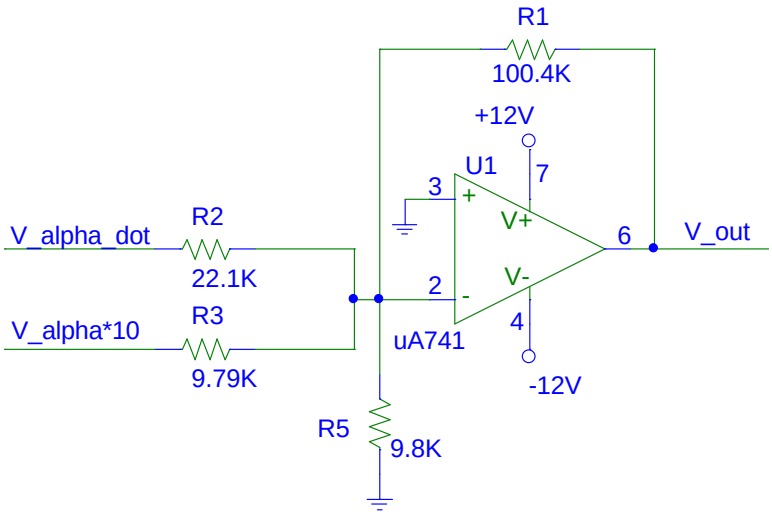

Figure A-2: The PD position controller used to hold the motor inertia at $\alpha = 0$ when mounting the pendulum.

within 1% through a range of 340°. Since the MATLAB model indicated that the system was sensitive to noise in the measurement of the pendulum angle, it was decided to power the β pot with a 5V voltage regulator, which filters much of the noise from the 12V power supply. With the regulator voltage of 4.94V, the potentiometer gain for the β pot, K_{bp}, is

$$K_{bp} = \frac{4.94V}{340^\circ} = 0.01453V/^\circ \tag{A.1}$$

The β pot was wired as one side of a wheatstone bridge circuit, as shown in Figure A-3. The primary reasons for choosing this circuit were the ability to obtain a positive and negative signal from a single voltage regulator, the potential to filter out common mode noise, and the convenience of being able to balance the circuit with a simple adjustment of the balancing pot, R_8. With the resistor values used in Figure A-3, this circuit was able to adjust the zero position of β through a wide angle and alleviate much concern about the orientation of the β pot during mounting.

After mounting the β pot and zeroing the wheatstone bridge, the output voltage difference $(V_a - V_b)$ is directly proportional to β. In order to reference this voltage

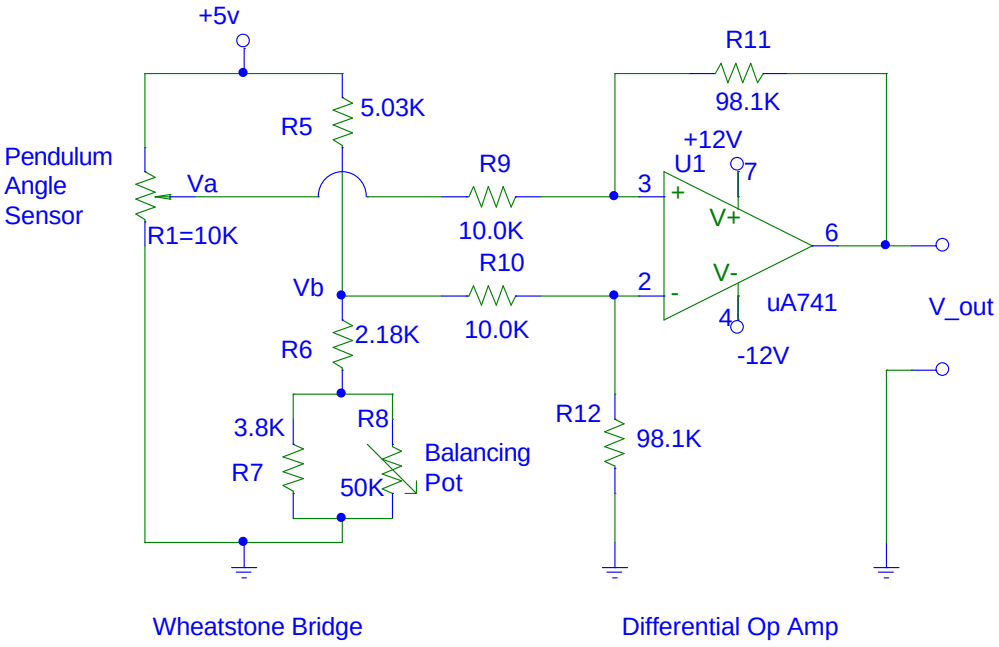

Figure A-3: The pendulum angle measurement was obtained by placing the potentiometer measuring β in a wheatstone bridge circuit and then using a differential amplifier to amplify the signal and reference it to ground.

difference to ground for use in the rest of the control circuit, the voltage output of the wheatstone bridge was passed through a differential amplifier, as shown in the right in Figure A-3. With $R_9 = R_{10} = 10.0\text{K}\Omega$ and $R_{11} = R_{12} = 98.1\text{K}\Omega$, the differential amplifier obeys the following relation

$$V_{out} = \frac{R_{11}}{R_{10}}(V_a - V_b) = 9.81(V_a - V_b) \tag{A.2}$$

where V_{out} is referenced to ground and the expected gain of the bridge circuit, K_b, due to the differential amplifier, is 9.81. This prediction corresponds very well with the measured gain of 9.8147, plotted in Figure A-4.

A.4 Differentiator Circuit for $\dot{\beta}$

In keeping with the minimalist approach to this this stabilization problem, the angular velocity of the pendulum, $\dot{\beta}$, was obtained by differentiating the position signal

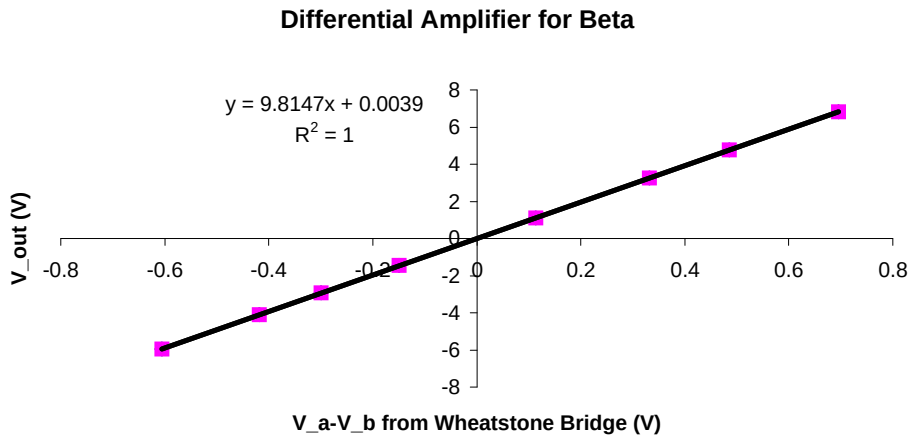

Figure A-4: The gain of the differential amplifier agreed well with the theory and was very linear.

obtained as in Section A.3. Figure A-5 shows the circuit designed to differentiate β.

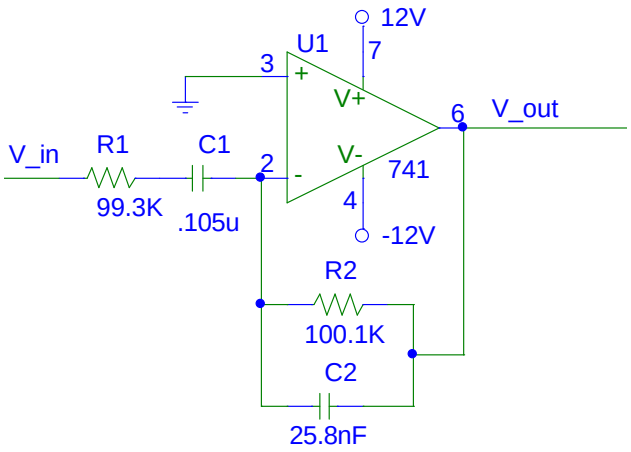

Figure A-5: This circuit was used to differentiate the angular position, β, to obtain the angular velocity, $\dot{\beta}$.

The transfer function for this differentiator circuit is

$$\frac{V_{out}(s)}{V_{in}(s)} = \frac{-R_2C_1s}{(R_1C_1s+1)(R_2C_2s+1)} \tag{A.3}$$

where the break frequencies are designed at $1/R_1C_1 = 95.9\text{rad/sec} = 15.3\text{Hz}$ and $1/R_2C_2 = 352\text{rad/sec} = 56.0\text{Hz}$. The upper break frequency was chosen to help

eliminate high frequency noise and the lower bound break frequency high enough to capture our expected response.

Figure A-6 plots the theoretical bode plot for this transfer function using MATLAB's `bode` function as well as the experimental data collected for the actual circuit. The resulting circuit differentiates well up to 15Hz, although the gain does not follow the theory exactly below approximately 2Hz.

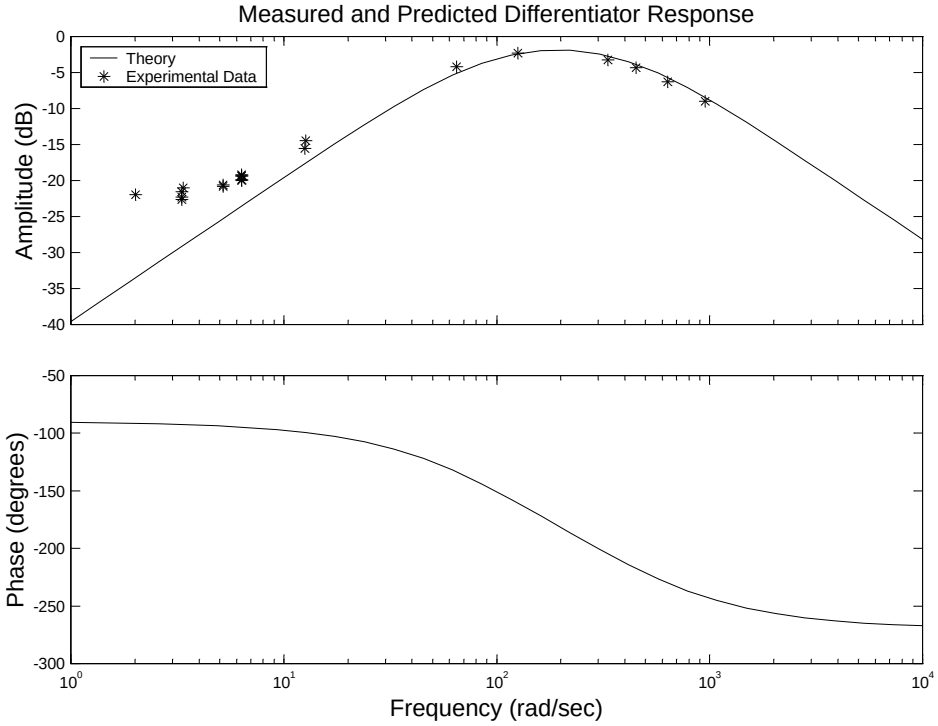

Figure A-6: The differentiator circuit performs close to the theory at higher frequencies but not so well at low frequencies.

A.5 Dead Zone Compensation Circuit

Testing demonstrated that the dead zone overwhelmed the control signal. Since the control system has no way of compensating for this non-linearity in the motor, a separate circuit was designed to try to compensate for the dead zone of the motor.

The dead zone was measured by slowly increasing the voltage into the servo am-

plifier and observing the minimum voltage required to make the motor turn. This voltage was found to be approximately -0.08V in the $-\alpha$ direction and 0.12V in the $+\alpha$ direction. These values correspond to torques of -0.027Nm and 0.040Nm, respectively, which seems reasonable given that in Smith and Sobhani found the value of the coulomb friction torque, T_f, to be 0.031Nm [3]. The asymmetry found here was also present in other motors tested and accounted well for the observed asymmetric behavior of the system.

The simple compensation scheme employed here is to "preload" the output signal. Essentially, we desire a circuit to perform the following math operation, which, if the compensating voltages were known exactly, should effectively remove the dead zone:

$$V_{out} = \begin{cases} V_{in} + 0.12\text{V if } V_{in} > 0 \\ V_{in} - 0.08\text{V if } V_{in} < 0 \end{cases}$$

Figure A-7 shows the circuit used to compensate for this asymmetric dead zone. Because, the voltage offset effect of the dead zone is fairly small, the circuit actually operates on the desired voltage amplified by a factor of ten, adding an offset voltage of 1.2V or -0.8V as appropriate and then reducing the signal by a factor of ten to obtain the desired output[1]. The first two op-amps in Figure A-7 serve as a simple comparator and inversion, which determine the sign of the input signal, causing V_s to be high (≈ 10.5V) when V_{in} is positive and low (≈ -10.5V) when V_{in} is negative.

The interesting part of this circuit is the voltage divider input to the third op-amp. This divider is designed such that when V_s is high the offset voltage, V_{off} is 1.20V and when V_s is low V_{off} is -0.80V. The resistor values given to achieve this are approximate. In the physical implementation a 10K potentiometer was used in place of R_4 and R_5. This pot was adjusted such that, without V_s connected, V_{off} was midway between the positive and negative offset voltages, here 0.2V. A 50K pot was then used in place of resistor R_3 and adjusted such that the desired positive

[1]This amplification and deamplification could be a problem if we reach the saturation limits of the op amps. In this case, if our desired output signal exceeds ≈ 1V, this amplification would have saturated the op amp, resulting in some loss of the signal. Fortunately, our control signals were low enough that this did not become a problem.

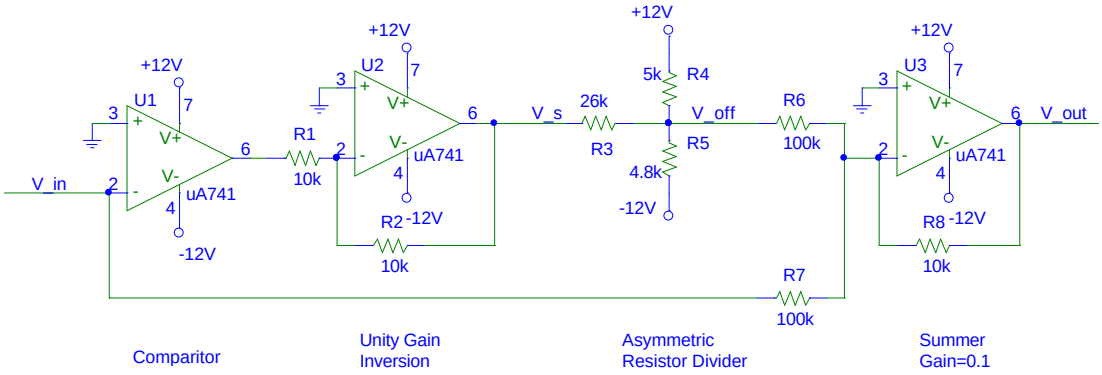

Figure A-7: This circuit was designed to compensate for the asymmetric dead zone of the motor.

and negative offset voltages were correct. This calibration was necessary because the voltage rails and the saturation output of the op amps vary with the power supply and op amps used, making a precise calculation of the resistor values tedious and unnecessary.

The last op amp simply sums the offset voltage to the original signal and then divides by ten to compensate for the earlier amplification by ten. The result of implementing this circuit was to improve symmetry in the response, but still the system was far from stable.

Appendix B

MATLAB Code

Below is given the MATLAB code used in the simulations of the pendulum. The file `thesis_init.m` initializes all the necessary constants as well as the state space matrices $\mathbf{A}, \mathbf{B}, \mathbf{C}$ and $\mathbf{D}$. The file `poleplacement.m` uses Ackermann's formula to obtain the state feedback gain matrix, $\mathbf{K}$. Finally the file `Kz_system`, modifies $\mathbf{K}$ to account for the system gains due to sensors and hardware in the system considered. The full simulink model used, `ziapenddemo.mdl`, is shown here in Figure B-1. The modifications to MATLAB's pendulum animation `pendan.m` is given, as well as the file `plot_penddemo.m`, which was used to plot the output response of the pendulum.

B.1 Initialization

```
%thesis_init.m
%This file initialized the values of all constants in the system.

global A B step num

L=.0532; %m
m=.0636; %kg
R=.0725; %m, base of pendulum from motor axis
g=9.81;  %m/sec^2

b=0.004; %hinge damping, adjusted for testing
c=0;    %Friction in the motor was determined to be coulomb only
```

```
        % so viscous coefficient is zero

%%%%%%Begin Dynamics for Rotary Base%%%%%

%Calculate the total inertia:
M=.05338; %Mass of the pendulum base bracket
R_clamp=.0375; %m
M_clamp=.2106; %Mass of the clamp (kg)
J=9.97e-4; %kg*m^2 inertia of the motor
I=J+M_clamp*R_clamp^2; %kgm^2, total inertia

%Input A and B matrices for pendulum with arcing base
den=M*R^2+I; %The common denominator of all terms
A_arc=[0 1 0 0; M*g*R/den -c/den -m*g*R/den b*R/(L*den); 0 0 0 1;
g*(I-M*R*L)/(L*den) c*(R+L)/(L*den) g*((M+m)*R^2+I+m*L*R)/(L*den)
-b*(((M+m)*R^2+I)/(m*L)+R)/(L*den)]

B_arc=[0; 1/den; 0; -(R+L)/(L*den)]

%% Initialize the A, B, C and D matrices for Simulink and poleplacement
A=A_arc;
B=B_arc;
C_all=eye(4); %Full state feedback
D=zeros(4,1);

%Simulink Constants:

Ka=1.9368; %Amplifier Gain A/V
Km=.1697; %Nm/A
Kf=.0306; %kg*m^2/sec^2, Coulomb friction coefficient
Kt=.0286; %V/(rad/sec)
Kp=.2504; %V/rad
Kbp=.014529; %calculated theoretical v/degree of beta pot
Kbp=Kbp*180/pi; %V/rad
Kd=0.0105; %R2C1
Kb=9.8147; %Gain differential amplifier after wheatstone bridge
Tzf=0;  %initialize dead zone to zero

step=0.0022; %initialize step input magnitude for signal generator
num=1000; %length of the output vector
```

B.2 Poleplacement

```
%poleplacement.m
%
%This file uses Ackermann's Formula to determine the K matrix.
%It also calls thesis_init and Kz_system, so running poleplacement.m
%sets up everything necessary to run the simulink file ziapenddemo.mdl

global A B

thesis_init;

M=[B A*B A*A*B A*A*A*B];
rank(M) %Rank of the M matrix needs to be 4 for this
        %system to be fully state controllable
%ans =
%
%     4

% Establish the Desired Characteristic Equation/closed loop poles
J=[-2+1.5*i 0 0 0;0 -2-1.5*i 0 0; 0 0 -10 0; 0 0 0 -10]

% Use Ackermann's Formula to find the Feedback matrix K, that
% will yield the desired closed loop poles and print K' to screen:
phi=polyvalm(poly(J), A);
K=[0 0 0 1]*inv(M)*phi;
K_transpose=K'

%Run the file Kz_system, which factors out the system gains and then
%print to screen the gains to be implemented in K_summer
Kz_system;
systemgain=Kz_sys'
```

B.3 Calculate System Gains

The following code modified the **K** matrix found using Ackermann's Formula to compensate for the system gains. For example, all of the control signals pass through the servo amplifier and the motor, thus, in the first step, the entire gain matrix is divided by K_a and K_m. This process is continued for each individual control signal to obtain

the system gain matrix, $\mathbf{K_{sys}}$.

```
%Kz_system
%
%Determine the system gain constant Kz_sys from the poleplacement result for K

Kz_sys=K/Km/Ka;  %These are the gains common to all inputs

                                %Gain adjustments for specific signals
Kz_sys(1)=Kz_sys(1)/Kp;         %alpha
Kz_sys(2)=Kz_sys(2)/Kt;         %alpha_dot
Kz_sys(3)=Kz_sys(3)/Kbp/Kb;     %beta
Kz_sys(4)=Kz_sys(4)/Kbp/Kb/Kd;  %beta_dot
```

B.4 Full Simulink Model

The full Simulink model used is shown in Figure B-1. The input and output blocks including the graphical animation came from MATLAB's Simulink example file on the inverted pendulum, `penddemo.mdl`, which can found by typing `penddemo` at the MATLAB prompt. The graphical output for the pendulum response was invaluable for quick observations of the system stability. The detailed pendulum response was plotted by outputting the system states to the workspace. These states were stored in the vector, y, while the time was stored in t.

B.5 Pendulum Animation

MATLAB's pendulum animiation was modifed to make the output image reflect the inverted pendulum with a rotary base. In the file `pendan.m` the following changes were made to the function `LocalPendSets`:

```
function LocalPendSets(time,ud,u)
%%%%%%%Modified Code%%%%%%
%u(2) ALPHA
%u(3) BETA
```

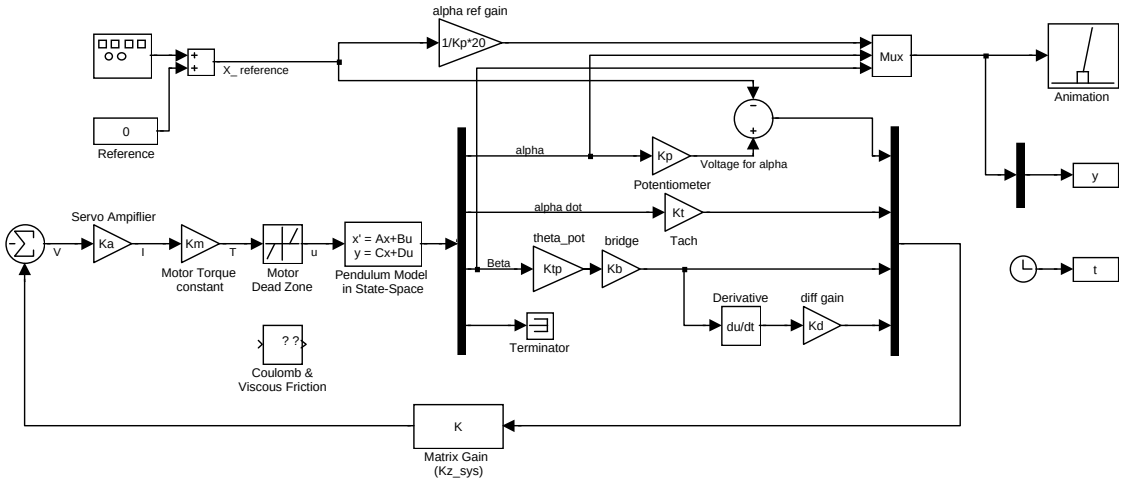

Figure B-1: The Full Simulink Pendulum Model.

```
%THETA=u(2)+u(3)
XDelta     = 0.2; %width of the base block
PDelta     = 0.2; %width of the pendulum
R          = 3;
L          = 4;
arrowwidth = 2;
XBaseTop = R*sin(u(2));
YBaseTop = R*cos(u(2));
PDcosA = XDelta*cos(u(2));
PDsinA = -XDelta*sin(u(2));

XPendTop = L*sin(u(3)+u(2))+XBaseTop;
YPendTop = L*cos(u(3)+u(2))+YBaseTop;
PDcosT   = PDelta*cos(u(3));
PDsinT   = -PDelta*sin(u(3));
 set(ud.Cart,...
   'XData', [XBaseTop-PDcosA XBaseTop+PDcosA; -PDcosA PDcosA],...
   'YData', [YBaseTop-PDsinA YBaseTop+PDsinA; -PDsinA PDsinA]);
set(ud.Pend,...
  'XData',[XPendTop-PDcosT XPendTop+PDcosT;...
    XBaseTop-PDcosT XBaseTop+PDcosT], ...
  'YData',[YPendTop-PDsinT+YBaseTop YPendTop+PDsinT+YBaseTop;...
    -PDsinT+YBaseTop PDsinT+YBaseTop]);
set(ud.TimeField,...
  'String',num2str(time));
set(ud.RefMark,...
   'XData',u(1)+[-arrowwidth 0 arrowwidth]);
```

```
%%%%%%%Modified Code%%%%%%%%

%%%%Original Code%%%%%%%
%XDelta   = 2; %width of the base block
%PDelta   = 0.2; %width of the pendulum
%XPendTop = u(2) + 12*sin(u(3));
%YPendTop = 12*cos(u(3));
%PDcosT   = PDelta*cos(u(3));
%PDsinT   = -PDelta*sin(u(3));
%set(ud.Cart,...
%  'XData',ones(2,1)*[u(2)-XDelta u(2)+XDelta]);
%set(ud.Pend,...
%  'XData',[XPendTop-PDcosT XPendTop+PDcosT; u(2)-PDcosT u(2)+PDcosT], ...
%  'YData',[YPendTop-PDsinT YPendTop+PDsinT; -PDsinT PDsinT]);
%set(ud.TimeField,...
%  'String',num2str(time));
%set(ud.RefMark,...
%  'XData',u(1)+[-XDelta 0 XDelta]);
%%%%%Original Code%%%%%%

% Force plot to be drawn
pause(0) drawnow

% end LocalPendSets
```

B.6 Plotting Output

The following code plotted the data collected in the output vector y during simulations.

```
%plot_penddemo.m
%
%plot ziapenddemo response

close all;
hold on;
subplot(2,1,1),
plot(t, y(:,2)*180/pi, 'b:',t, y(:,3)*180/pi, 'b-')

ylabel('Angle (degrees)');
title('Response of the Pendulum');
```

```
legend('Alpha','Beta')

subplot(2,1,2),plot(t, (y(:,2)+y(:,3))*180/pi,'b-');

xlabel('Time (sec)');
ylabel( 'Angle (degrees)');
legend('Theta');
```

Bibliography

[1] Horowitz, Paul and Winfield Hill. *The Art of Electronics*. 2nd ed. Cambridge, Eng.: Cambridge University Press, 2001.

[2] Ogata, Katsuhiko. *Modern Control Engineering*. 3rd ed. Upper Saddle River, NJ: Prentice-Hall, 1997.

[3] Smith, Adiel and Ziaieh Sobhani. Data collected in MIT's 2.010 Lab. Spring, 2001.